Title
Regulation of glottal closure and airflow in a three-dimensional phonation model: Implications for vocal intensity control

Journal
The Journal of the Acoustical Society of America, 137(2)

ISSN
0001-4966

Author
Zhang, Zhaoyan

Publication Date
2015-02-01

DOI
10.1121/1.4906272

Peer reviewed

Regulation of glottal closure and airflow in a three-dimensional phonation model: Implications for vocal intensity control

Zhaoyan Zhang[a)]
UCLA School of Medicine, 31-24 Rehabilitation Center, 1000 Veteran Avenue, Los Angeles, California 90095-1794

(Received 22 September 2014; revised 23 November 2014; accepted 8 December 2014)

Maintaining a small glottal opening across a large range of voice conditions is critical to normal voice production. This study investigated the effectiveness of vocal fold approximation and stiffening in regulating glottal opening and airflow during phonation, using a three-dimensional numerical model of phonation. The results showed that with increasing subglottal pressure the vocal folds were gradually pushed open, leading to increased mean glottal opening and flow rate. A small glottal opening and a mean glottal flow rate typical of human phonation can be maintained against increasing subglottal pressure by proportionally increasing the degree of vocal fold approximation for low to medium subglottal pressures and vocal fold stiffening at high subglottal pressures. Although sound intensity was primarily determined by the subglottal pressure, the results suggest that, to maintain small glottal opening as the sound intensity increases, one has to simultaneously tighten vocal fold approximation and/or stiffen the vocal folds, resulting in increased glottal resistance, vocal efficiency, and fundamental frequency. © *2015 Acoustical Society of America*.
[http://dx.doi.org/10.1121/1.4906272]

[ADP] Pages: 898–910

I. INTRODUCTION

Maintaining a small mean glottal opening during phonation is important for several reasons. First, a small glottal opening enhances the glottal fluid-structure interaction and thus lowers the phonation threshold pressure, making it easier to initiate phonation. Second, a small glottal opening is associated with high glottal resistance (GR). With a sufficiently high GR the desired subglottal pressure or vocal intensity can be established with less glottal flow, which is essential to maintaining a normal duration of speech between breaths and low respiratory efforts. Finally, reduced glottal flow also reduces noise production due to turbulence. Thus, one may argue that maintaining a small glottal opening and low flow rate is one of the posturing goals of normal voice production. Indeed, human subjects studies have shown that the mean glottal flow during phonation remains relatively constant (around 100–200 ml/s) across a large range of subglottal pressures as vocal intensity increases (Isshiki, 1964; Hirano, 1981; Tanaka and Gould, 1983; Holmberg *et al.*, 1988; Stathopoulos and Sapienza, 1993). In some conditions, the mean glottal flow even decreased slightly with increasing intensity in the experiments of Isshiki (1964) and Holmberg *et al.* (1988). On the other hand, an excessively large flow rate is often an indication of pathological changes that presumably create a large glottal opening during phonation.

But how is such a low flow rate maintained relatively constant across a large range of subglottal pressures during normal phonation? With fixed material properties and geometry, the vocal folds would be pushed apart with increasing subglottal pressure, as demonstrated in the excised larynx experiment by van den Berg and Tan (1959). Clearly, some laryngeal adjustments of vocal fold properties (stiffness, tension, geometry, and position) are required in order to restrain the vocal folds from being pushed apart by airflow. Despite many previous studies on the effect of laryngeal adjustments on phonation, both in humans (e.g., Isshiki, 1964, 1969; Hirano *et al.*, 1969; Gay *et al.*, 1972; Choi *et al.*, 1993) and three-dimensional simulations (Titze and Talkin, 1979; Alipour *et al.*, 2000; Zheng *et al.*, 2011; Xue *et al.*, 2012; Sidlof *et al.*, 2013), the interaction between the subglottal pressure and laryngeal adjustments of vocal fold properties in regulating glottal closure and airflow has not been systematically investigated.

From a mechanical point of view, the glottis-opening effect of the subglottal pressure can be counterbalanced by either tightening vocal fold approximation or vocal fold stiffening. Our previous studies explored the possible effects of vocal fold stiffening in maintaining glottal closure against the subglottal pressure (Zhang, 2011; Xuan and Zhang, 2014). The effect of vocal fold approximation was not considered in these studies because of experimental observations that vocal fold approximation alone without simultaneous stiffening in isotropic models is insufficient to maintain vocal fold position against the subglottal pressure and often leads to an excessively large glottal opening and flow rate (Zhang, 2011; Mendelsohn and Zhang, 2011). However, human vocal folds are inherently anisotropic, due to the presence of collagen and elastin fibers along the anterior-posterior (AP) direction. Recent studies (Xuan and Zhang, 2014; Zhang, 2014) suggest that an inherently anisotropic vocal fold may be able to better maintain its position against the subglottal pressure. Thus, one may wonder, for anisotropic vocal folds as in humans, if a typical mean glottal flow rate can be maintained by adjusting the degree of vocal

a)Author to whom correspondence should be addressed. Electronic mail: zyzhang@ucla.edu

fold approximation alone without extra vocal fold stiffening, at least for low subglottal pressures or conversational conditions. If so, how much approximation of the vocal folds is required to achieve a glottal flow rate typical of normal phonation for a given subglottal pressure? And beyond what subglottal pressure is simultaneous vocal fold stiffening required and how much stiffening is required?

Understanding the degree of vocal fold approximation and stiffening required to maintain a small glottal opening and low flow rate at different subglottal pressures would provide insights toward the roles of individual laryngeal muscle activation in voice control. In humans, while the lateral cricoarytenoid (LCA) and the interarytenoid (IA) muscles are responsible for approximating the vocal folds, complete closure of the membranous portion of the vocal folds requires activation of the thyroarytenoid (TA) muscle (Choi *et al.*, 1993; Chhetri *et al.*, 2012; Yin and Zhang, 2014). Thus, the minimum degree of vocal fold approximation required for maintaining a typical glottal flow would clarify the possible roles of the LCA/IA/TA muscles in intensity control. The TA muscle also coordinates with the cricothyroid (CT) muscle in regulating vocal fold stiffness and tension. Therefore, these two muscles may also be recruited to provide the necessary restraining effect through vocal fold stiffening to balance the varying subglottal pressure. Such an improved understanding may provide new perspectives about why we control voice the way we do, if a matching between the restraining function and the subglottal pressure proves to be essential to producing normal voice. For example, it is well known that increasing subglottal pressure is often accompanied by a proportional increase in GR (Isshiki, 1964, 1969; Hirano *et al.*, 1969; Tanaka and Tanabe, 1986; Holmberg *et al.*, 1988; Stathopoulos and Sapienza, 1993) but the underlying reason is unclear. It is possible that, as subglottal pressure increases, vocal fold approximation and stiffening must also increase to maintain the desired glottal opening and a small flow rate, thus increasing GR.

The goal of the present study was to investigate the interaction among the subglottal pressure, initial glottal width (degree of vocal fold approximation), and vocal fold stiffness in the regulation of the mean glottal area and flow rate, and its effects on the intensity and frequency of the produced voice. The focus on the initial glottal width and vocal fold stiffness as intermediate control variables bridging physiology and vibration is clinically important because an important goal of clinical management of voice disorders is to restore the mechanical state of the vocal folds required for normal phonation. Although laryngeal muscle activation affects vocal fold stiffness in all directions, Yin and Zhang (2013) showed that stiffness along the AP direction exhibited the largest variation with varying CT/TA activations. Thus, this study specifically focused on the interaction among vocal fold stiffness along the AP direction, the subglottal pressure, and the initial glottal width, using a reduced-order three-dimensional vocal fold model. The use of a reduced-order model is necessary considering the large number of conditions to be investigated and the high computational costs if a fully resolved model were used. In the following, the reduced-order numerical model is first described in Sec. II. Typical results from this model are also shown and compared to available human data. The interaction between vocal fold AP stiffness, initial glottal width, and subglottal pressure is then discussed in Sec. III, followed by a general discussion in Sec. IV.

II. METHOD

A. Numerical model

Figure 1 shows the three-dimensional vocal fold model used in this study. For simplicity, left–right symmetry in vocal fold geometry and vibration about the glottal midline was imposed so that only one vocal fold was considered in this study with the contralateral fold exhibiting mirror-image motion. Extension of the model to left–right asymmetric conditions is straightforward as in Zhang and Luu (2012). For simplicity, the vocal fold model was further assumed to have a uniform cross-sectional geometry along the AP direction, as in many previous studies of phonation (e.g., Scherer *et al.*, 2001; Zheng *et al.*, 2011; Bhattacharya and Siegmund, 2013). The cross-sectional geometry of the vocal fold model was defined similarly as in Zhang (2009, Fig. 2). The vocal fold model was fixed at the lateral surface and the two side surfaces at the anterior and posterior ends.

Although the vocal fold is physiologically a multilayered structure and often simplified as a body-cover two-layer structure, Yin and Zhang (2013) showed that CT/TA activations generally led to a varying difference between the AP and transverse stiffnesses but not much stiffness difference between the body and cover layers. In other words, the vocal folds behaved mechanically as a one-layer structure for most CT/TA conditions. Thus, in this study, the vocal fold was modeled as a one-layer transversely isotropic, nearly incompressible, linear material with a plane of isotropy perpendicular to the AP direction, as in previous studies (Titze and Talkin, 1979; Itskov and Aksel, 2002; Zhang, 2011, 2014). The material control parameters for the transversely-isotropic vocal fold included the transverse Young's modulus E_t, the AP Young's modulus E_{ap}, the AP shear modulus G_{ap}, and density. The longitudinal Poisson's

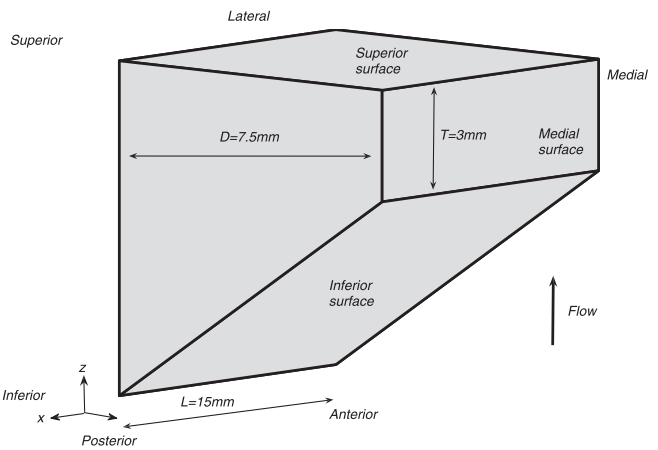

FIG. 1. The three-dimensional vocal fold model. The flow direction is along the positive z axis. The coupled vocal folds-flow system was assumed to be symmetric about the glottal channel centerline so that only one vocal fold was considered in this study.

ratio was assumed to be 0.495. To reduce the number of conditions to be investigated, $E_{ap} = 4\ G_{ap}$ was further assumed in this study. The vocal fold was coupled to a one-dimensional flow model, as described in detail in the Appendix. No sub- or supra-glottal tracts were included in this study to avoid possible source-tract interactions.

It is noted that the vocal folds are known to have nonlinear material properties, and large deformations of the vocal fold may occur, particularly during vocal fold posturing. Thus, the material moduli used in this study should be interpreted as the tangent moduli around certain vocal fold posturing conditions, with different stiffness values representing different posturing conditions (e.g., different degrees of elongation due to CT muscle activation). The use of a linear elastic material also implicitly assumed small-strain deformations, which may not be valid for very large-amplitude vocal fold vibrations.

The different stiffness conditions considered in this study were summarized in Table I. As this study focused on the effect of the AP stiffness, the AP shear modulus G_{ap} was varied in a large range to encompass possible physiological range. Note that the minimum value of G_{ap} in Table I was 6 kPa, below which no phonation was observed for the subglottal pressure range investigated (up to 2.4 kPa). Examination of vocal fold deformation in these conditions (i.e., $G_{ap} < 6$ kPa, corresponding to isotropic or small degree of anisotropy) showed large static deformation, which may have violated the small-strain assumption, and these conditions were thus not included in the discussion below. The transverse Young's modulus in the range of 2–4 kPa was considered, similar to previous studies (Titze and Talkin, 1979; Berry *et al.*, 1994) and experimental measurement (Chhetri *et al.*, 2011). The initial glottal width was varied in a range between −0.4 and 1 mm, with the negative values for conditions of vocal folds being pressed against each other at rest.

B. Data analysis

Data analysis was performed using the last 0.25 s of each simulation at which vocal fold vibration had reached steady-state or nearly steady-state. In addition to the mean glottal area Ag_0 and mean glottal flow rate Q_{mean}, the glottal area amplitude Ag_t was calculated as the difference between maximum and minimum glottal areas. The sound pressure level (SPL) was calculated as the root-mean-square value of the produced sound 30 cm away from the glottal exit. A similar measure was also calculated for the noise component of the voices. The GR was calculated as the ratio between the subglottal pressure and the mean glottal flow rate. Vocal efficiency was calculated as the ratio between the radiated sound power and the product of the subglottal pressure and the mean flow rate.

C. Model validation

Direct validation of the numerical model by comparing to experiments is difficult due to lack of well-controlled experiments with anisotropic physical vocal fold models. Human and animal larynges are anisotropic, but the lack of reliable methods for measurement of the anisotropic material properties and geometry indicates most of the model input parameters have to be estimated, preventing direct quantitative validation. Thus, in this section, typical results from our numerical model are presented, with the goal of demonstrating that this model was able to produce vibration patterns and phonation characteristics similar to what has been reported in humans.

Figures 2 and 3 show vocal fold vibration within one oscillation cycle from the superior view and in the coronal plane, as well as the time history of a medial-lateral slice taken from the superior view images over a few oscillation cycles (also known as kymograms). The vocal fold had a small AP stiffness ($G_{ap} = 6$ kPa) in Fig. 2 and a relatively large AP stiffness ($G_{ap} = 18$ kPa) in Fig. 3, while the subglottal pressure was the same at 2.4 kPa. In each figure, the first frame of the superior-view images roughly corresponds to the instant of maximum glottal opening. Both figures exhibit many vibratory features that are considered typical of normal phonation. The glottis showed alternating open and closed phases. During the opening phase, the vocal folds were pushed slightly upwards and had a convergent medial surface shape. The vocal folds moved downward during the closing phase, with the medial surface forming a divergent glottis. There was a vertical phase difference in vibration along the medial surface, with the lower margin leading in phase, which is often considered an important feature of normal phonation (Titze, 1994, Chap. 4). As a result, vocal fold contact started at the lower margin of the medial surface and propagated upwards along the medial surface then to the superior surface. This laterally-propagating wave along the superior surface was clearly visible in the kymograms.

Noticeable differences can be also observed between the two conditions. The stiff vocal folds in Fig. 3 remained closed longer during one oscillation cycle, with a closed quotient of about 0.22, than the soft vocal folds in Fig. 2 which had a closed quotient of about 0.08. The soft folds also exhibited a much larger vertical displacement compared with the stiff folds and had a number eight shaped glottis during opening, both of which were reported in previous

TABLE I. Simulation conditions. For all conditions, the vocal fold density was 1.2 kg/m^3, the AP Poisson's ratio was 0.495, and the length was 15 mm. Negative values of the initial glottal width indicate vocal fold compression.

Transverse Young's modulus	$E_t = [2, 4]$ kPa
AP shear modulus	$G_{ap} = [6, 8, 10, 12, 14, 16, 18, 20, 25, 30, 35, 40, 45]$ kPa
AP Young's modulus	$E_{ap} = 4\ G_{ap}$
Initial glottal width	$g_0 = [-0.4, -0.2, 0, 0.2, 0.4, 0.6, 1]$ mm
Subglottal pressure	$P_s = [0, 50, 100, 200, 300, 400, 500, 600, 700, 800, 1200, 1600, 2000, 2400]$ Pa

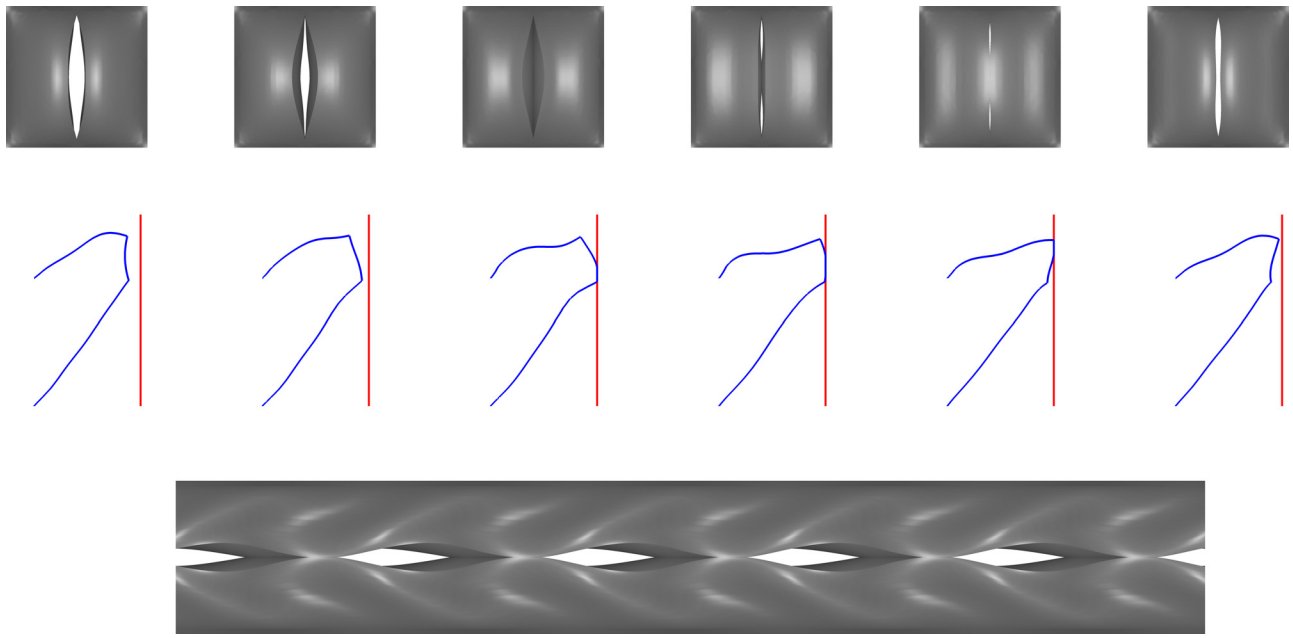

FIG. 2. (Color online) Vocal fold vibration for $G_{ap} = 6$ kPa. Top panel: Superior view of vocal fold vibration during one oscillation cycle; middle panel: Vocal fold surface shape in the coronal plane during one oscillation cycle (vertical lines indicate glottal midline); bottom panel: Time history of a medial-lateral slice located at the middle along the AP direction from the superior view of vocal fold vibration in the top panel, with time from left to right.

experiments (Mendelsohn and Zhang, 2011; Zhang, 2011; Murray and Thomson, 2012; Xuan and Zhang, 2014). The wave-like motion, particularly on the lateral surface, was also more obvious in Fig. 3 with an increased AP stiffness, which is consistent with the observation in Zhang (2014).

In the discussion below, we also show that the ranges of various aerodynamic and acoustic measures of phonation predicted by our model are comparable to those observed in humans. In addition, our previous studies using similar computational models have been able to reproduce experimental observations regarding sound production by confined pulsating jet flows (Zhang *et al.*, 2002), dependence of phonation threshold pressure on vocal fold properties (Mendelsohn and Zhang, 2011), vocal fold vibration patterns in different vibratory regimes, and transitions between regimes (Zhang and Luu, 2012; Zhang, 2014). Based on the above, we concluded that our model captured the essential features of glottal fluid-structure interaction and was sufficient for qualitative investigations of the regulation of glottal closure and flow rate in phonation.

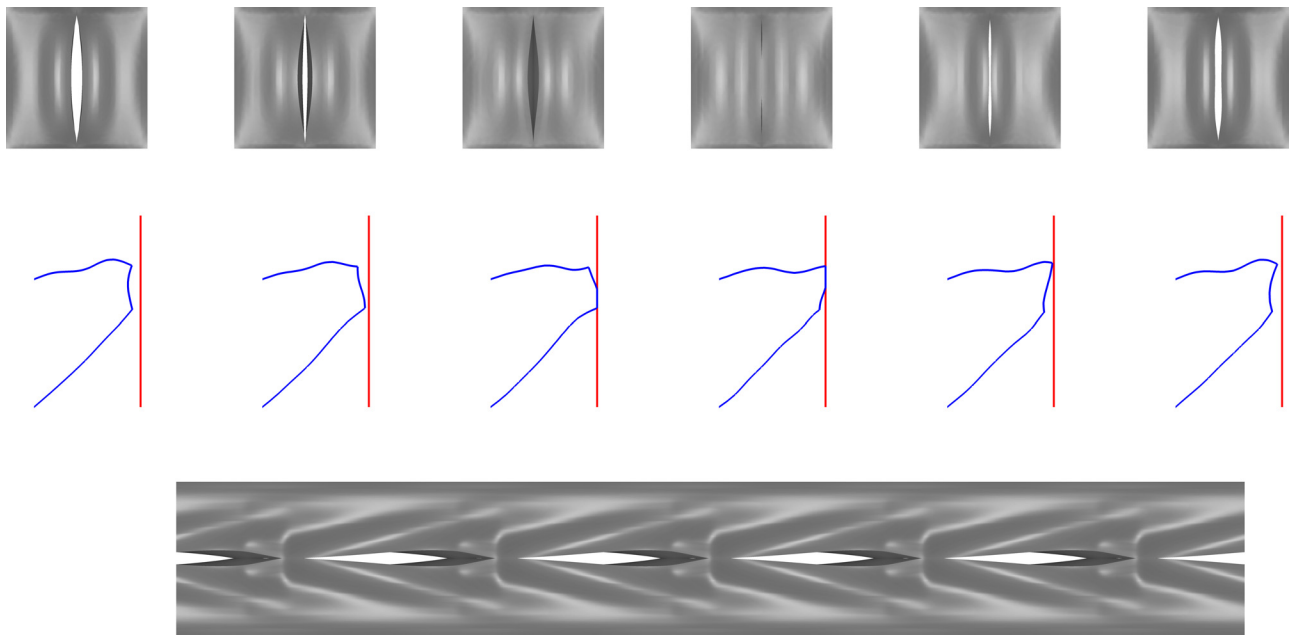

FIG. 3. (Color online) Vocal fold vibration for $G_{ap} = 18$ kPa. Top panel: Superior view of vocal fold vibration during one oscillation cycle; middle panel: Vocal fold surface shape in the coronal plane during one oscillation cycle (vertical lines indicate glottal midline); bottom panel: Time history of a medial-lateral slice located at the middle along the AP direction from the superior view of vocal fold vibration in the top panel, with time from left to right.

III. RESULTS

A. Effects of pressure-stiffness interaction

Figure 4 shows the different aerodynamic and acoustic measures as a function of the subglottal pressure and AP stiffness of the vocal fold, for conditions with a zero initial glottal width. Note that regions in the figure without data indicate conditions at which no phonation was observed or, in the case of noise level, no noise was produced. Due to this zero initial glottal width, phonation onset occurred at very low subglottal pressures (around 50–100 Pa). With increasing subglottal pressure, the vocal fold was gradually pushed open, resulting in an increase in both the mean glottal area and the mean flow rate. Increasing subglottal pressure also led to increased glottal area amplitude. Note that the mean glottal area during vibration (around 5 mm^2) was much smaller than that observed in isotropic models (around 20 mm^2; Mendelsohn and Zhang, 2011; Zhang, 2011), indicating a much improved capability of the vocal fold to resist deformation against the subglottal pressure. In contrast, increasing vocal fold AP stiffness had opposite effects from the subglottal pressure, reducing the mean glottal opening, the mean flow rate, and the glottal area amplitude. These effects of increasing AP stiffness were more significant at high subglottal pressures.

The fundamental frequency $F0$ in Fig. 4 was determined mainly by the AP stiffness, but also increased slightly with increasing subglottal pressure at low subglottal pressures. The SPL, in contrast, was primarily determined by the subglottal pressure. For the same subglottal pressure, the SPL remained almost constant (1–2 dB variation) with varying AP stiffness. This is a little surprising considering the decreased vibration amplitude with increasing AP stiffness. Further analysis of the glottal flow waveform showed that increasing AP stiffness also reduced the duration of the closing phase, probably due to the increase in $F0$. These two effects canceled out each other so that the maximum flow declination rate (negative peak of the time-derivative of the glottal flow, which is known to relate to sound intensity) and thus sound intensity remained almost constant across different values of the AP stiffness.

Due to the antagonistic effects of the subglottal pressure and AP stiffness in controlling the mean glottal opening and the mean flow rate, the GR increased with either decreasing subglottal pressure or increasing AP stiffness, with the subglottal pressure having a larger effect. Similarly, noise production increased with either increasing subglottal pressure or decreasing AP stiffness. Because the SPL was primarily determined by the subglottal pressure, the vocal efficiency showed a similar pattern as the GR, increasing with decreasing subglottal pressure and to a lesser extent with increasing AP stiffness.

B. Effects of initial glottal width

Similar antagonistic effects of the subglottal pressure and vocal fold AP stiffness in the control of the mean glottal flow and glottal area were observed for other initial glottal widths investigated, as shown in Fig. 5 for an initial glottal width of 0.4 mm. Increasing subglottal pressure still led to increases in both the mean glottal flow and mean glottal area whereas vocal fold stiffening reduced them. However, the effect of vocal fold stiffening in reducing the glottal area and flow decreased with increasing initial glottal width. This can be seen in Fig. 6(a), which shows the mean glottal flow rate as a function of the subglottal pressure for different initial glottal widths. For each initial glottal width in Fig. 6(a), the upper and lower curves correspond to conditions with the smallest AP stiffness ($G_{ap} = 6$ kPa) and largest AP stiffness ($G_{ap} = 45$ kPa), respectively, which also correspond to the maximum and minimum mean glottal flow rate possible for the specific subglottal pressure and initial glottal width. For an initial glottal width of zero and a subglottal pressure of

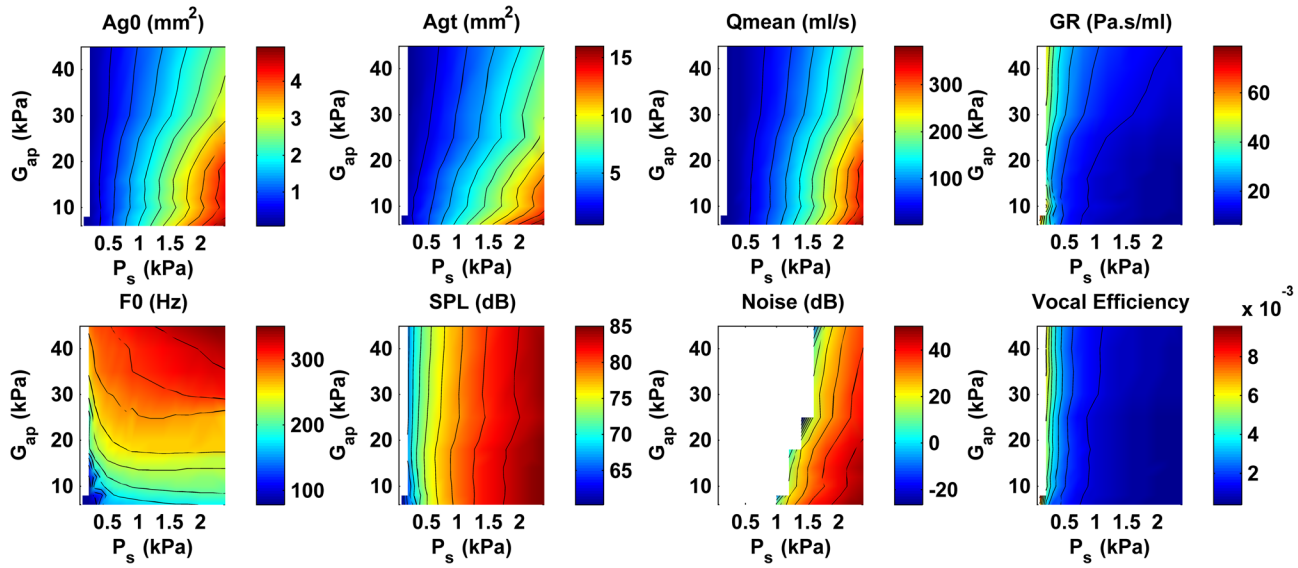

FIG. 4. (Color online) Different aerodynamic, acoustic, and vibrational measures as a function of the subglottal pressure (P_s) and vocal fold AP stiffness G_{ap}, for an initial glottal width $g_0 = 0$ mm. See Sec. II for definitions of different measures. Regions without data indicate conditions at which no phonation was observed or, in the case of the noise level, no noise was produced.

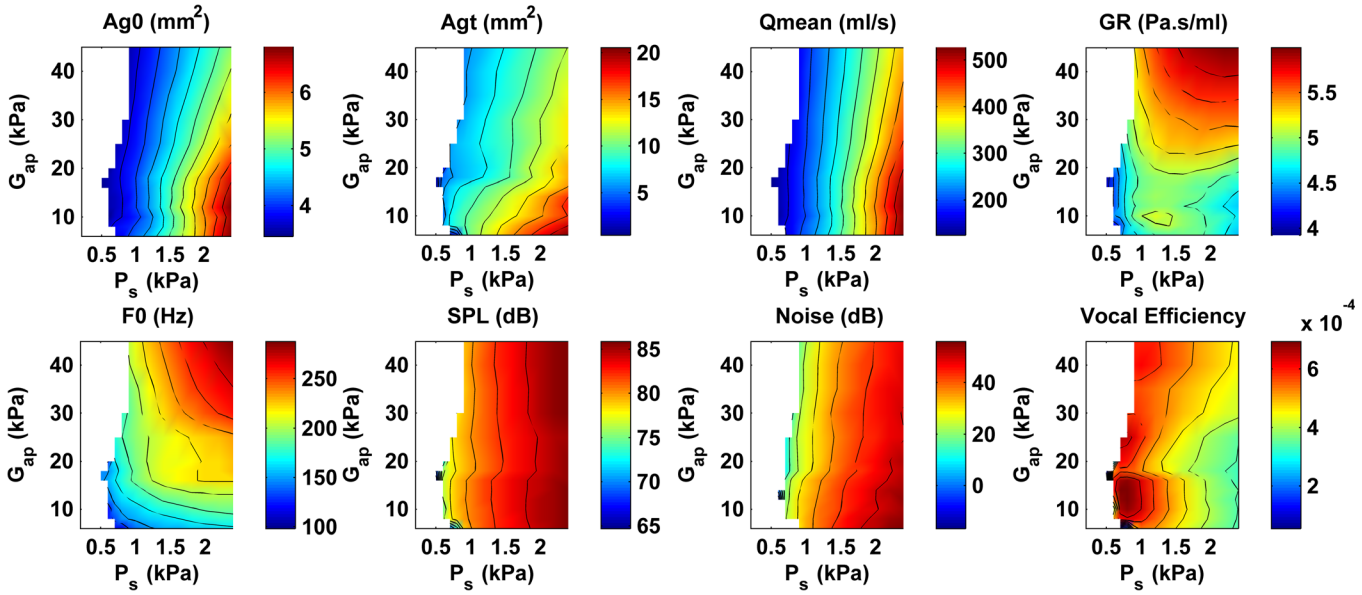

FIG. 5. (Color online) Different aerodynamic, acoustic, and vibrational measures as a function of the subglottal pressure (P_s) and vocal fold AP stiffness G_{ap}, for an initial glottal width $g_0 = 0.4$ mm. See Sec. II for definitions of different measures. Regions without data indicate conditions at which no phonation was observed or, in the case of the noise level, no noise was produced.

2.4 kPa, maximum vocal fold stiffening almost reduced the mean glottal flow by half, whereas this reduction was about 9% for an initial glottal width of 1 mm.

Figure 6(a) also shows that the glottis-opening effect of increasing subglottal pressure can be countered more effectively by reducing the initial glottal width, i.e., tightening vocal fold approximation. For example, for a subglottal pressure of 800 Pa, reducing the initial glottal width from 0.6 to 0.2 mm alone lowered the mean glottal flow rate from 237 to 116 ml/s, almost reduced by half. Figure 6(a) further shows that increasing vocal fold approximation was much more effective at low subglottal pressures than vocal fold stiffening. With increasing subglottal pressure, the flow-reducing effect of increasing vocal fold approximation remained almost constant whereas vocal fold stiffening became increasingly effective, particularly for small initial glottal widths.

On the other hand, Fig. 6(a) shows that tight vocal fold approximation was critical to maintaining a small mean flow rate. Increasing initial glottal width significantly increased the minimum mean glottal flow rate that was possible. For an initial glottal width of 0.2 mm, the lowest mean flow rate required for phonation was 47 ml/s. This value increased to about 470 ml/s for an initial glottal width of 1 mm, which is much higher than observed in normal human phonation. Thus, without sufficient vocal fold approximation (e.g., $g_0 > 0.4$ mm), it is impossible to maintain a mean glottal flow expected of normal phonation, with or without vocal fold stiffening [Fig. 6(a)].

The initial glottal widths also had a significant effect on the phonation threshold pressure, as shown in Fig. 6(b). The phonation threshold pressure decreased with decreasing initial glottal width, reached minimum around a zero initial glottal width, and then increased with further decrease in the initial glottal width (i.e., increasing vocal fold medial compression). Note that the maximum compression condition with a −0.4 mm initial glottal width is not shown in Fig. 6 because the corresponding phonation threshold pressure in this case was so high that no phonation was observed in the subglottal pressure range examined in this study (up to 2.4 kPa). Thus, although medial compression led to a maximum restraining effect [Fig. 6(a)], it also significantly increased the minimum pressure required to initial phonation. Figure 6(b) also shows that, for a given initial glottal width (except for the case of a zero initial glottal width), there was an optimal AP stiffness at which the phonation threshold pressure was the lowest.

Despite this large effect on the phonation threshold pressure, decreasing initial glottal width only slightly decreased the SPL [Fig. 6(c)], which appeared to depend primarily on the subglottal pressure, except for around phonation onset. As a result, the region of soft (low-intensity) voice production in the pressure-stiffness space was significantly reduced when the initial glottal width significantly deviated (either increase or decrease) from the zero value. In other words, production of soft voice became increasingly difficult with either a very open glottis or a tightly compressed glottis. Increasing initial glottal width also led to reduced range of fundamental frequency, especially at the upper end, as shown in Fig. 6(d).

Increasing initial glottal width significantly reduced both the GR [Fig. 6(e)] and vocal efficiency [Fig. 6(f)], mostly due to the increased mean flow rate. The variation patterns of the GR and vocal efficiency as a function of the subglottal pressure also varied with the initial glottal width. For conditions of zero or negative initial glottal width, both the GR and vocal efficiency decreased with increasing subglottal pressure, whereas for larger initial glottal widths, both measures first increased then decreased with increasing subglottal pressure.

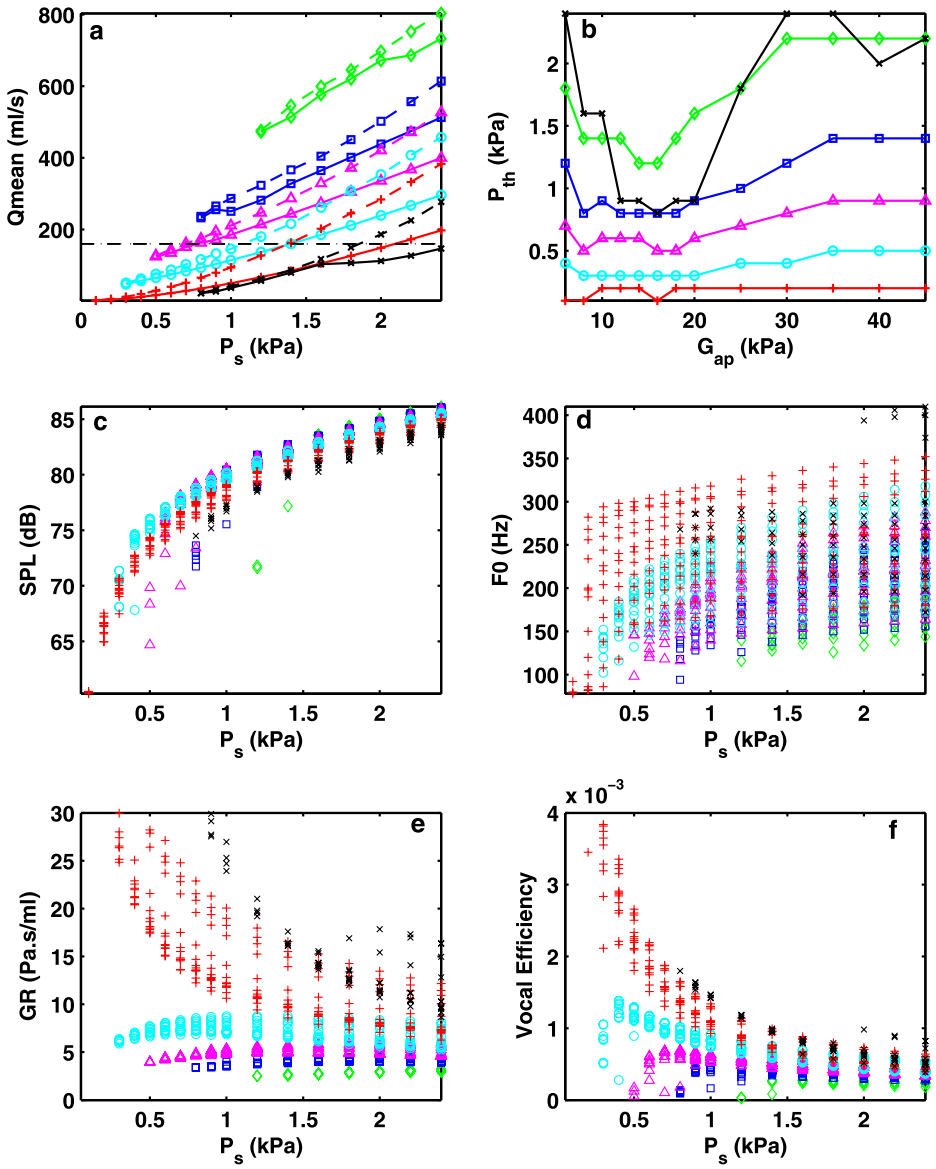

FIG. 6. (Color online) Effects of the initial glottal width for $E_t = 4$ kPa. (a) The mean glottal flow rate Q_{mean} as a function of the subglottal pressure and initial glottal width. For a clearer illustration, only data for the smallest ($G_{\text{ap}} = 6$ kPa, dashed lines) and largest AP stiffness ($G_{\text{ap}} = 45$ kPa, solid lines) are shown for each initial glottal width; (b) the phonation threshold pressure P_{th} as a function of AP stiffness G_{ap} for different initial glottal widths; (c) the SPL, (d) the phonation frequency, (e) the GR, and (f) the vocal efficiency as a function of the subglottal pressure (P_s) and initial glottal width, for all conditions of AP stiffness. ×: $g_0 = -0.2$ mm; +: $g_0 = 0$ mm; ○: $g_0 = 0.2$ mm; △: $g_0 = 0.4$ mm; □: $g_0 = 0.6$ mm; ◇: $g_0 = 1$ mm. The dashed-dotted line in Fig. 6(a) indicates the target flow rate of 160 ml/s as discussed in Sec. IV B.

C. Effects of vocal fold transverse stiffness

Figure 7 shows similar results obtained for conditions with a lower transverse stiffness E_t of 2 kPa. The general observations discussed above remained qualitatively the same. Decreasing the transverse stiffness of the vocal folds reduced the vocal fold's ability to maintain its position against the subglottal pressure. As a result, the mean glottal flow rate for a given subglottal pressure increased significantly with decreasing transverse stiffness. For example, for an initial glottal width of 0.4 mm and a subglottal pressure of 2 kPa, the maximum mean glottal flow rate increased from 421 to 721 ml/s as the transverse stiffness decreased from 4 to 2 kPa. On the other hand, vocal fold stiffening became more important in maintaining a low mean flow rate, especially for high subglottal pressures. For example, for the two conditions above, increasing the AP stiffness to 45 kPa was able to bring the mean flow rate down to almost the same level for the two transverse stiffness conditions (336 and 387 ml/s for a transverse stiffness of 4 and 2 kPa, respectively). The effect of medial compression also seemed to be reduced, with the conditions of 0 and −0.2 mm initial glottal widths having almost the same minimum mean flow rate possible.

Comparing Figs. 6(b) and 7(b) also shows that the transverse stiffness had a much larger effect than the AP stiffness on the phonation threshold pressure. The relatively smaller effect of the AP stiffness on phonation threshold pressure was probably due to its small effect on the frequency spacing between the first few *in vacuo* eigenmodes, an important determinant of the phonation threshold pressure (Zhang, 2011). Thus, vocal fold stiffening along the AP direction is more advantageous than stiffening in all directions as the restraining effect is achieved without much increase in the phonation threshold pressure.

IV. DISCUSSION AND CONCLUSIONS

A. Summary of results

This study confirmed a previous experimental observation that anisotropic vocal folds were better able to maintain

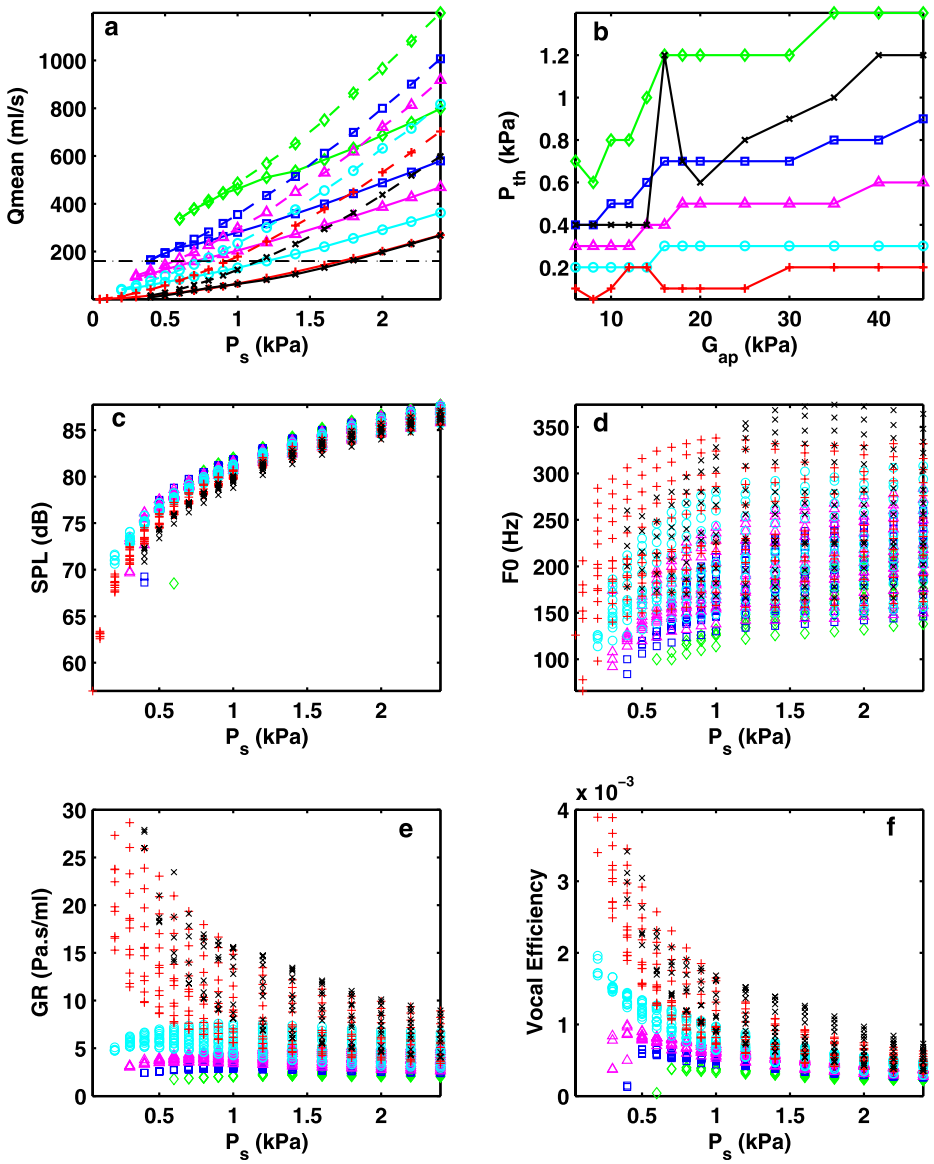

FIG. 7. (Color online) Effects of the initial glottal width for $E_t = 2$ kPa. (a) The mean glottal flow rate Q_{mean} as a function of the subglottal pressure and initial glottal width. For a clearer illustration, only data for the smallest ($G_{ap} = 6$ kPa, dashed lines) and largest AP stiffness ($G_{ap} = 45$ kPa, solid lines) are shown for each initial glottal width; (b) the phonation threshold pressure P_{th} as a function of AP stiffness G_{ap} for different initial glottal widths; (c) the SPL, (d) the phonation frequency, (e) the GR, and (f) the vocal efficiency as a function of the subglottal pressure (P_s), and the initial glottal width, for all conditions of AP stiffness. ×: $g_0 = -0.2$ mm; +: $g_0 = 0$ mm; ○: $g_0 = 0.2$ mm; △: $g_0 = 0.4$ mm; □: $g_0 = 0.6$ mm; ◇: $g_0 = 1$ mm. The dashed-dotted line in (a) indicates the target flow rate of 160 ml/s as discussed in Sec. IV B.

their position against the subglottal pressure (Zhang, 2011, 2014; Xuan and Zhang, 2014). Although the vocal folds were still pushed open with increasing subglottal pressure, the increase in the mean glottal area and flow rate decreased with increasing vocal fold AP stiffening (i.e., increasing anisotropy) and were much smaller than those observed in isotropic models. With this improved capability of maintaining position, a small glottal opening and a relatively constant mean flow can be maintained against increasing subglottal pressure by a proportional increase in vocal fold approximation alone without extra vocal fold stiffening. We further showed that increasing vocal fold approximation was more effective in reducing the glottal flow at low to medium subglottal pressures whereas vocal fold stiffening became increasingly more effective at high subglottal pressures.

Sound intensity was found to depend primarily on the subglottal pressure, which was consistent with the observation in Tanaka and Tanabe (1986). For a given subglottal pressure (and a constant vocal fold geometry), changes in vocal fold stiffness or initial glottal width had only a slight effect on sound intensity. However, increasing vocal fold approximation and stiffening did significantly increase the GR, which would facilitate establishing the desired subglottal pressure without an excessively large glottal flow and thus maintaining a normal duration of speech between breaths. Thus, although an increase in the GR was often observed to accompany intensity increase in humans (Isshiki, 1964), it does not increase sound intensity by itself. It appears that the GR is increased simply to achieve the subglottal pressure required for such intensity increase while still maintaining a small glottal opening and a low glottal flow rate, as further demonstrated in Sec. IV B.

The results of this study also showed that neither a large glottal opening nor a very tightly compressed glottis is desirable for phonation. A large initial glottal width, as in the case of recurrent laryngeal nerve paralysis or vocal fold atrophy, increases the demand for subglottal pressure (increased phonation threshold pressure) when at the same time it reduces the capability to maintain a normal glottal flow rate of phonation (because of reduced GR). This results in a large glottal flow, which reduces the possible duration of speech between breaths and increases the respiratory effort required. In the extreme case, one may suffer from reduced loudness

range as it becomes difficult to achieve and maintain sufficient subglottal pressure required for a loud voice long enough for continuous speech. On the other hand, a tightly compressed glottis, as in the case of adductory spasmodic dysphonia, significantly increased phonation threshold pressure, thus requires an excessively high lung pressure to even initial phonation. At the extreme cases, the compression may be too tight that phonation becomes impossible (e.g., $g_0 = -0.4$ mm in this study). Finally, because of the high phonation threshold pressure, soft voice production becomes difficult for either a large glottal opening or a very tightly compressed glottis.

B. Implications for human voice control: Balance between subglottal pressure and glottal resistance

The mean flow rate in normal human phonation is in the range between 60 and 340 ml/s, with the average ranging from 120 to 200 ml/s (Hirano, 1981; Holmberg *et al.*, 1988; Stathopoulos and Sapienza, 1993). To demonstrate the effects of maintaining a small glottal flow rate on phonation, we consider a target mean flow rate of 160 ml/s and $E_t = 4$ kPa. Figure 8(a) (the symbols) shows the minimum degree of vocal fold stiffening required to maintain a flow rate at or below the target level, for a given subglottal pressure and initial glottal width. The corresponding mean flow rate was shown in Fig. 8(b). Note that tight vocal fold approximation with g_0 at least 0.4 mm (or initial glottal area of 6 mm^2) is required to maintain such low flow rate (thus to appear in Fig. 8), similar to observations in Isshiki (1989, 1998). If we consider a larger initial glottal width as requiring less laryngeal efforts (i.e., less laryngeal muscle activation), an optimal posturing route with the least laryngeal effort can be determined by choosing, for each subglottal pressure, the posture with the largest initial glottal width yet still capable of maintaining a flow rate below 160 ml/s. Following this optimal posturing route (lines in Fig. 8), the low intensity sound does not require extra vocal fold stiffening, and only medium approximation is required ($g_0 = 0.4$ mm in this case, except for the lowest intensity sound which requires tight but not compressed vocal fold approximation). As the target sound intensity increases, in addition to an increase in the subglottal pressure, the degree of vocal fold approximation must also be increased. For subglottal pressures above around 1.4 kPa, simultaneous vocal fold stiffening is required to further increase sound intensity while still maintaining a flow rate below 160 ml/s. Thus, in order to maintain a small glottal flow rate, an increase in sound intensity necessarily requires a simultaneous increase in the GR [Fig. 8(e); first due to increased vocal fold approximation then increased vocal fold stiffening], although sound intensity was primarily controlled by the subglottal pressure [Fig. 8(c)]. Increasing sound intensity in this way also led to an increase in the fundamental frequency and vocal efficiency. Such a simultaneous increase in GR and vocal efficiency with increasing sound intensity has also been observed in the human subjects experiment by Isshiki (1964). Note that the predicted values of the GR in Fig. 8(e) are also comparable to those reported in Isshiki (1964).

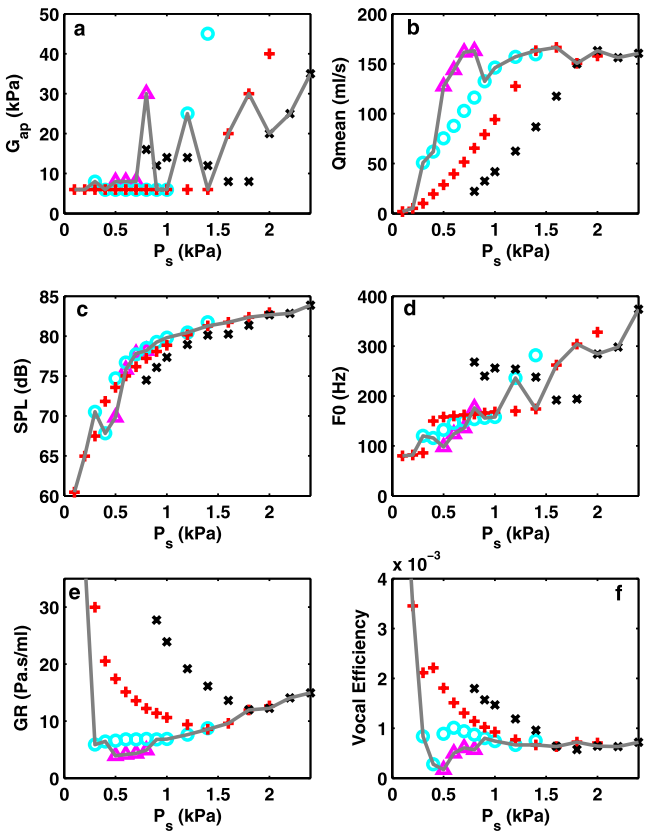

FIG. 8. (Color online) (a) The AP stiffness required to maintain a mean glottal flow below 160 ml/s and (b) the corresponding mean glottal flow rate, (c) SPL, (d) fundamental frequency, (e) the GR, and (f) vocal efficiency as a function of the subglottal pressure. ×: $g_0 = -0.2$ mm; +: $g_0 = 0$ mm; ○: $g_0 = 0.2$ mm; △: $g_0 = 0.4$ mm; —: the optimal posturing with the least laryngeal effort.

In humans, although the LCA and IA muscles are responsible for bringing the vocal folds close to each other, *in vivo* canine larynx experiments (Choi *et al.*, 1993; Chhetri *et al.*, 2012) showed that LCA/IA activation alone is unable to completely close the mid-membranous glottis and activation of the TA muscle is required to completely close the mid-membranous glottis. A rough estimation of the mid-membranous glottal width at maximum LCA/IA activation alone from Choi *et al.* (1993) is about 0.5–1 mm, whereas a recent numerical study (Yin and Zhang, 2014) predicted a mid-membranous glottal width around 0.8 mm. Thus, while LCA/IA activation alone is able to provide the minimum vocal fold approximation required (0.4 mm in this study), it is the TA muscle whose activation provides the fine adjustment in the degree of vocal fold approximation required to maintain small glottal opening and a glottal flow rate typical of normal phonation against the varying subglottal pressure. On the other hand, the AP stiffness of the vocal folds is generally assumed to be regulated primarily by the CT muscle. Thus, according to Fig. 8, to increase vocal intensity, in addition to LCA/IA activation, one may initially rely on TA activation to increase the degree of vocal fold approximation at low–medium subglottal pressures, and then increase CT activation for high subglottal pressures. This is consistent with a previous observation that activity of the TA muscle was positively correlated with vocal intensity for low pitches in chest register (Hirano *et al.*, 1969, 1970).

However, the TA and CT muscles are known to have antagonistic effects on both vocal fold approximation and vocal fold stiffening. Activation of the CT muscle at some conditions may also abduct the vocal folds (van den Berg and Tan, 1959), whereas TA activation may also shorten the vocal fold and reduce AP stiffness (Hirano, 1974; Yin and Zhang, 2013). These antagonistic effects of the CT/TA muscles indicate that, as the sound intensity is increased from low to high, at some point one has to switch from a TA-dominant posture at low-to-medium subglottal pressures to a CT-dominant posture at high subglottal pressures. Our results showed that such a switch is more likely to occur at a high subglottal pressure when TA deactivation is required to reach maximum stiffening. Such deactivation of the TA muscle at high pitches has been observed in previous human subject studies (Hirano *et al.*, 1969, 1970). The point of switch depends on the stiffness conditions (the transverse stiffness, comparing Figs. 6 and 7) and contact properties (which determine medial compression's effect on phonation threshold pressure). Because the fundamental frequency is primarily controlled by the CT muscle (see, e.g., Chhetri *et al.*, 2012), such a switch is likely to lead to an abrupt jump in fundamental frequency and possible voice quality changes similar to those observed in register changes, a possibility which requires further investigation.

C. Limitations and future work

The limitations of this study lie in the simplifications made in the numerical model, including simplified vocal fold geometry and simplified physics in both the flow and structure models. One major simplification is the neglect of material and geometric nonlinearity in the vocal fold model. These simplifications were necessary to reduce the computational costs required for parametric studies involving a large number of conditions as in this study, but they may be inadequate for certain aspects of phonation. For example, it is possible that inclusion of the nonlinear effects will lead to a much larger increase in phonation frequency with increasing subglottal pressure than observed in this study. Use of a large-displacement large-strain formulation would also require more accurate data of the material properties of the vocal folds (both soft tissue layer and the muscle layer), another direction needing further attention. Also, the glottal flow has been known to exhibit many complex features (Neubauer *et al.*, 2007; Sidlof *et al.*, 2011), which may need to be included in future flow models. However, despite these simplifications, our previous studies using similar computational models have been able to qualitatively reproduce experimental observations (Zhang *et al.*, 2002; Mendelsohn and Zhang, 2011; Zhang and Luu, 2012; Zhang, 2014), and thus it is reasonable to assume this model captures the essential features of the glottal fluid-structure interaction and the general conclusions of this study are qualitatively applicable to human phonation. Nevertheless, this study needs to be repeated using a more realistic vocal fold model or in experiments in future investigations.

Human phonation often involves an opening in the cartilaginous portion of the glottis, which was not modeled in this study. The presence of this posterior opening will lead to a baseline glottal flow throughout the entire oscillation cycle, in the presence of which stronger approximation and/or stiffening in the membranous vocal folds are required if the same mean flow rate were to be maintained.

As discussed above, in humans, the initial glottal width and vocal fold stiffness are not independent from each other as both are controlled by the same set of laryngeal muscles. Laryngeal muscle activation may also lead to simultaneous changes in vocal fold geometry, e.g., the medial surface shape, changes of which may significantly affect the glottal fluid-structure interaction (Hirano *et al.*, 1970; Titze, 1994). Future work will focus on using a muscular model (e.g., Yin and Zhang, 2014) to link muscular activities to vocal fold stiffness, tension, geometry, and position so that the interaction between laryngeal muscle activation and the varying subglottal pressure and its effect on phonation can be properly understood.

ACKNOWLEDGMENTS

This study was supported by research Grant Nos. R01 DC011299 and R01 DC009229 from the National Institute on Deafness and Other Communication Disorders, the National Institutes of Health.

APPENDIX: DETAILS OF THE NUMERICAL MODEL

A. Vocal fold model

The vocal fold displacement vector U was approximated as linear superposition of the *in vacuo* eigenmodes of the vocal folds

$$U(X_0,t)=\sum_{i=1}^{N} q_i(t)\varphi_i(X_0), \tag{A1}$$

where φ_i is the displacement vector of the ith *in vacuo* normalized eigenmode of the vocal fold, q_i is the ith generalized coordinate, $X_0=[x_0,\ y_0,\ z_0]$ is the position vector of vocal fold surface at the resting condition, and N is the number of eigenmodes included in the numerical simulation. In this study, $N=40$ was used. The instantaneous vocal fold surface position $X=[x,\ y,\ z]$ was calculated as

$$X(X_0,t)=X_0+U(X_0,t). \tag{A2}$$

The governing equations of the vocal folds were derived from Lagrange's equations as

$$M\ddot{q}+C\dot{q}+Kq=Q, \tag{A3}$$

where M, C, and K are the mass, damping, and stiffness matrices of the vocal fold structure, respectively, and Q is the generalized force vector associated with the intraglottal pressure and contact pressure. The mass and stiffness matrices M and K were defined as

$$M_{ij}=\frac{\partial}{\partial\ddot{q}_j}\left(\frac{d}{dt}\left(\frac{\partial L}{\partial\dot{q}_i}\right)\right);\quad K_{ij}=\frac{\partial}{\partial q_j}\left(-\frac{\partial L}{\partial q_i}\right), \tag{A4}$$

where Lagrangian $L=V-U$. The associated kinetic energy V and potential energy U of the vocal fold structure were defined similarly to that in Zhang *et al.* (2007). The generalized force Q was calculated as

$$Q_k = -\int_{S_{FSI}} \left((p+p_c)\frac{\partial U}{\partial q_k}\cdot n \right) dS, \quad k=1,2,\ldots,N, \tag{A5}$$

where S_{FSI} denotes the fluid-structure interface of the vocal fold with the normal vector n pointing outward from the vocal fold volume, p and p_c are the flow pressure and contact pressure acting on the fluid-structure interface, which were calculated based on the instantaneous glottal area and the imposed subglottal pressure as described below.

In this study, a constant loss factor σ of 0.4 was used, similar to previous studies (e.g., Zhang, 2009). With the assumptions of a linear elastic material and small-strain deformation, the use of the normalized *in vacuo* eigenmodes as the basis functions in Eq. (A1) simplifies the mass, damping, and stiffness matrices in Eq. (A3) to diagonal matrices, with the diagonal elements given as below,

$$M_{ii}=1; \quad K_{ii}=\omega_i^2; \quad C_{ii}=\sigma\omega_i, \tag{A6}$$

where ω_i is the ith *in vacuo* angular eigenfrequency.

Note that, although the vocal fold eigenmodes contained information of the three-dimensional motion within the vocal fold volume, only the motion on vocal fold surface was required in calculating the glottal flow pressure and solving Eq. (A3). In this study, the vocal fold eigenmodes were calculated using the commercial software COMSOL.

B. Glottal flow model

The glottal flow was assumed to be a one-dimensional quasi-steady potential flow until it separated from the glottal wall at a location downstream of the minimum glottal constriction where the glottal area was 1.2 times the minimum glottal area. Downstream of the flow separation point the pressure was assumed to equal to atmospheric pressure or pressure at the entrance to the vocal tract if present. The intraglottal pressure p at a location within the glottis with a cross-sectional area $A(z)$ was given by

$$p = p_{sup} + \frac{1}{2}\rho u_j^2\left(1-\frac{A_j^2}{A^2}\right), \tag{A7}$$

where ρ is the density of air, p_{sup} is the instantaneous supra-glottal pressure immediately above the glottis, and A_j and u_j are the glottal area and flow velocity of the jet formed at the flow separation point. The jet velocity was calculated as described in Sec. D below. The instantaneous glottal opening area at a superior-inferior location z was calculated by integrating the glottal width along the vocal fold surface contour $l(z)$,

$$A(z,t) = 2\int_{l(z)} \max(0,(y_{midline}-y))dl, \tag{A8}$$

where $y_{midline}$ is the y-coordinate of the glottal midline along the medial-lateral direction. The factor of 2 appears due to the imposed left–right symmetry in vocal fold vibration.

Noise production due to turbulent flow developed downstream of the glottis was modeled by adding an additional component $u_{j,noise}$ to the instantaneous jet velocity, similar to previous studies (e.g., Samlan and Story, 2011),

$$u_{j,noise}A_j = \begin{cases} 1\times10^{-12}N_{noise}(\mathrm{Re}^2-\mathrm{Re}_{crit}^2), & \mathrm{Re}>\mathrm{Re}_{crit} \\ 0, & \text{otherwise,} \end{cases} \tag{A9}$$

where N_{noise} is a random variable with a uniform distribution between -0.5 and 0.5. The Reynolds number $\mathrm{Re}=u_jA_j/(L\nu)$, where L is vocal fold length and ν is the dynamic viscosity of air. For this study, Re_{crit} was set to 1200 as in Samlan and Story (2011).

C. Vocal fold contact model

Due to the imposed left–right symmetry in vocal fold vibration, vocal fold collision was considered to occur when the vocal fold crossed the glottal midline, in which case a contact pressure along the medial-lateral direction into the vocal fold was applied to the contact area on vocal fold surface. The contact pressure was related to the degree the vocal fold crossed the midline, similar to Ishizaka and Flanagan (1972),

$$p_c = k_{c1}\omega_1^2(y_{midline}-y)[1+k_{c2}\omega_1^2(y_{midline}-y)^2], \quad \text{if } y>y_{midline}, \tag{A10}$$

where ω_1 is the first *in vacuo* angular eigenfrequency of the vocal fold, and k_{c1} and k_{c2} are two contact coefficients. In this study, k_{c1} and k_{c2} were set to 600 and 6000, respectively, so that the calculated contact pressure was in the range as measured in Jiang and Titze (1994).

D. Acoustic propagation within the sub- and supra-glottal tracts

Although no vocal tract was considered in this study, coupling between vocal fold vibration to the sub- and supra-glottal tracts is included here for completeness of the model description. Only plane-wave sound propagation was considered, which is generally valid for frequencies up to 4–5 kHz depending on the cross-sectional dimension of the sub- and supra-glottal tracts. A digital waveguide model as described in Story (1995) was used, in which the acoustic pressure and velocity within the tracts were decomposed into a forward-propagating (away from the glottis) wave f and a backward-propagating (toward the glottis) wave b,

$$p_a(z,t) = f(z,t)+b(z,t); \quad u_a(z,t) = \frac{f(z,t)}{\rho c} - \frac{b(z,t)}{\rho c}, \tag{A11}$$

where c is the speed of sound. The acoustic model was coupled to the glottal flow model in a similar way as described in Titze (1984) and Zhang *et al.* (2002), by relating the acoustic velocities and the glottal flow velocities at the entrance and exit of the glottis:

$$f_s - b_s = -\frac{A_j}{A_{\text{ent}}}\rho c u_j; \quad f_{\text{sup}} - b_{\text{sup}} = \frac{A_j}{A_{\text{exit}}}\rho c u_j, \tag{A12}$$

where the subscripts "*s*" and "*sup*" indicate the values evaluated at locations immediately below (sub-) and above (supra-) the glottis, respectively. The jet velocity can be obtained by solving Eqs. (A7) and (A12), similar to Titze (1984),

$$u_j = \frac{-A_j c\left(\frac{1}{A_{\text{ent}}} + \frac{1}{A_{\text{exit}}}\right)}{1 - \frac{A_j^2}{A_{\text{ent}}^2}} + \sqrt{\frac{A_j^2 c^2 \left(\frac{1}{A_{\text{ent}}} + \frac{1}{A_{\text{exit}}}\right)^2}{\left(1 - \frac{A_j^2}{A_{\text{ent}}^2}\right)^2} + \frac{2(P_s - P_{\text{sup}} + 2b_s - 2b_{\text{sup}})}{\rho\left(1 - \frac{A_j^2}{A_{\text{ent}}^2}\right)}}. \tag{A13}$$

E. Time-domain integration

Equation (A3) was solved using a fourth-order Runge-Kutta procedure, with a time step of 2.27×10^{-5} s (or 44 100 Hz). A zero initial condition was imposed for all three components of vocal fold displacement, the glottal flow velocity, and the acoustic pressure and velocity in the vocal tract. The subglottal pressure P_s was first linearly increased from zero to a target value in 30 time steps, and then kept constant. For each condition, simulation was run for 0.5 s. In all simulation conditions, by the end of this half-second simulation, vocal fold vibration either had already reached steady state or completely damped out.

Alipour, F., Berry, D. A., and Titze, I. R. (**2000**). "A finite-element model of vocal-fold vibration," J. Acoust. Soc. Am. **108**, 3003–3012.

Berry, D. A., Herzel, H., Titze, I. R., and Krischer, K. (**1994**). "Interpretation of biomechanical simulations of normal and chaotic vocal fold oscillations with empirical eigenfunctions," J. Acoust. Soc. Am. **95**, 3595–3604.

Bhattacharya, P., and Siegmund, T. (**2013**). "A computational study of systematic hydration in vocal fold collision," Comput. Methods Biomech. Biomed. Eng. **17**(16), 1835–1852.

Chhetri, D., Neubauer, J., and Berry, D. (**2012**). "Neuromuscular control of fundamental frequency and glottal posture at phonation onset," J. Acoust. Soc. Am. **131**(2), 1401–1412.

Chhetri, D. K., Zhang, Z., and Neubauer, J. (**2011**). "Measurement of Young's modulus of vocal fold by indentation," J. Voice **25**, 1–7.

Choi, H., Berke, G., Ye, M., and Kreiman, J. (**1993**). "Function of the thyroarytenoid muscle in a canine laryngeal model," Ann. Otol., Rhinol. Laryngol. **102**, 769–776.

Gay, T., Hirose, H., Strome, M., and Sawashima, M. (**1972**). "Electromyography of the intrinsic laryngeal muscles during phonation," Ann. Otol. Rhinol. Laryngol. **81**, 401–409.

Hirano, M. (**1974**). "Morphological structure of the vocal fold and its variations," Folia Phoniatr. **26**, 89–94.

Hirano, M. (**1981**). *Clinical Examination of Voice: Disorders of Human Communication* (Springer, New York), Chap. 3.

Hirano, M., Ohala, J., and Vennard, W. (**1969**). "The function of laryngeal muscles in regulating fundamental frequency and intensity of phonation," J. Speech Hear. Res. **12**, 616–628.

Hirano, M., Vennard, W., and Ohala, J. (**1970**). "Regulation of register, pitch and intensity of voice: An electromyographic investigation of intrinsic laryngeal muscles," Folia Phoniat. **22**, 1–20.

Holmberg, E., Hillman, R., and Perkell, J. (**1988**). "Glottal airflow and transglottal air pressure measurements for male and female speakers in soft, normal, and loud voice," J. Acoust. Soc. Am. **84**, 511–529.

Ishizaka, K., and Flanagan, J. L. (**1972**). "Synthesis of voiced sounds from a two-mass model of the vocal cords," Bell Syst. Tech. J. **51**, 1233–1267.

Isshiki, N. (**1964**). "Regulatory mechanism of voice intensity variation," J. Speech Hear. Res. **7**, 17–29.

Isshiki, N. (**1969**)."Remarks on mechanism for vocal intensity variation," J. Speech Hear. Res. **12**, 669–672.

Isshiki, N. (**1989**). *Phonosurgery: Theory and Practice* (Springer-Verlag, Tokyo), Chap. 3.

Isshiki, N. (**1998**). "Mechanical and dynamical aspects of voice production as related to voice therapy and phonosurgery," J. Voice **12**, 125–137.

Itskov, M., and Aksel, N. (**2002**). "Elastic constants and their admissible values for incompressible and slightly compressible anisotropic materials," Acta Mech. **157**, 81–96.

Jiang, J. J., and Titze, I. R. (**1994**). "Measurement of vocal fold intraglottal pressure and impact stress," J. Voice **8**, 132–144.

Mendelsohn, A., and Zhang, Z. (**2011**). "Phonation threshold pressure and onset frequency in a two-layer physical model of the vocal folds," J. Acoust. Soc. Am. **130**, 2961–2968.

Murray, P. R., and Thomson, S. L. (**2012**). "Vibratory responses of synthetic, self-oscillating vocal fold models," J. Acoust. Soc. Am. **132**, 3428–3438.

Neubauer, J., Zhang, Z., Miraghaie, R., and Berry, D. A. (**2007**). "Coherent structures of the near field flow in a self-oscillating physical model of the vocal folds," J. Acoust. Soc. Am. **121**, 1102–1118.

Samlan, R. A., and Story, B. H. (**2011**). "Relation of structural and vibratory kinematics of the vocal folds to two acoustic measures of breathy voice based on computational modeling," J. Speech, Lang., Hear. Res. **54**, 1267–1283.

Scherer, R., Shinwari, D., De Witt, K., Zhang, C., Kucinschi, B., and Afjeh, A. (**2001**). "Intraglottal pressure profiles for a symmetric and oblique glottis with a divergence angle of 10 degrees," J. Acoust. Soc. Am. **109**(4), 1616–1630.

Sidlof, P., Doare, O., Cadot, O., and Chaigne, A. (**2011**). "Measurement of flow separation in a human vocal folds model," Exp. Fluids **51**, 123–136.

Sidlof, P., Horacek, J., and Ridky, V. (**2013**). "Parallel CFD simulation of flow in a 3D model of vibrating human vocal folds," Comput. Fluids **80**, 290–300.

Stathopoulos, E., and Sapienza, C. (**1993**). "Respiratory and laryngeal function of women and men during vocal intensity variation," J. Speech Hear. Res. **36**, 64–75.

Story, B. H. (**1995**). "Physiologically-based speech simulation using an enhanced wave-reflection model of the vocal tract," Ph.D. dissertation, University of Iowa, Chap. 2.

Tanaka, S., and Gould, W. (**1983**). "Relationships between vocal intensity and noninvasively obtained aerodynamic parameters in normal subjects," J. Acoust. Soc. Am. **73**(4), 1316–1321.

Tanaka, S., and Tanabe, M. (**1986**). "Glottal adjustment for regulating vocal intensity: An experimental study," Acta Otolaryngol. **102**, 315–324.

Titze, I. R. (**1984**). "Parameterization of glottal area, glottal flow and vocal fold contact area," J. Acoust. Soc. Am. **75**(2), 570–580.

Titze, I. R. (**1994**). *Principles of Voice Production* (Prentice-Hall, Inc., Englewood Cliffs, NJ), Chaps. 4 and 10.

Titze, I., and Talkin, D. (**1979**). "A theoretical study of the effects of various laryngeal configurations on the acoustics of phonation," J. Acoust. Soc. Am. **66**, 60–74.

van den Berg, J. W., and Tan, T. S. (**1959**). "Results of experiments with human larynxes," Pract. Otorhinolaryngol. **21**, 425–450.

Xuan, Y., and Zhang, Z. (**2014**). "Influence of embedded fibers and an epithelium layer on glottal closure pattern in a physical vocal fold model," J. Speech, Lang., Hear. Res. **57**, 416–425.
Xue, Q., Zheng, X., Mittal, R., and Bielamowicz, S. (**2012**). "Computational modeling of phonatory dynamics in a tubular three dimensional model of the human larynx," J. Acoust. Soc. Am. **132**, 1602–1613.
Yin, J., and Zhang, Z. (**2013**). "The influence of thyroarytenoid and cricothyroid muscle activation on vocal fold stiffness and eigenfrequencies," J. Acoust. Soc. Am. **133**, 2972–2983.
Yin, J., and Zhang, Z. (**2014**). "Interaction between the thyroarytenoid and lateral cricoarytenoid muscles in the control of vocal fold adduction and eigenfrequencies," J. Biomech. Eng. **136**(11), 111006.
Zhang, Z. (**2009**). "Characteristics of phonation onset in a two-layer vocal fold model," J. Acoust. Soc. Am. **125**, 1091–1102.
Zhang, Z. (**2011**). "Restraining mechanisms in regulating glottal closure during phonation," J. Acoust. Soc. Am. **130**, 4010–4019.
Zhang, Z. (**2014**). "The influence of material anisotropy on vibration at onset in a three-dimensional vocal fold model," J. Acoust. Soc. Am. **135**(3), 1480–1490.
Zhang, Z., and Luu, T. (**2012**). "Asymmetric vibration in a two-layer vocal fold model with left-right stiffness asymmetry: Experiment and simulation," J. Acoust. Soc. Am. **132**(3), 1626–1635.
Zhang, Z., Mongeau, L., and Frankel, S. H. (**2002**). "Experimental verification of the quasi-steady approximation for aerodynamic sound generation by pulsating jets in tubes," J. Acoust. Soc. Am. **112**(4), 1652–1663.
Zhang, Z., Neubauer, J., and Berry, D. A. (**2007**). "Physical mechanisms of phonation onset: A linear stability analysis of an aeroelastic continuum model of phonation," J. Acoust. Soc. Am. **122**(4), 2279–2295.
Zheng, X., Mittal, R., and Bielamowicz, S. (**2011**). "A computational study of asymmetric glottal jet deflection during phonation," J. Acoust. Soc. Am. **129**(4), 2133–2143.